Inorganic Chemistry

Article

pubs.acs.org/IC

Methane to Methanol Conversion Induced by Thorium Oxide through the $CH_3Th(O)H$ Intermediate in Solid Argon

Yu Gong,[†] Lester Andrews,*[,†] Virgil E. Jackson,[‡] and David A. Dixon*[,‡]

[†]Department of Chemistry, University of Virginia, Charlottesville, Virginia 22904-4319, United States

[‡]Department of Chemistry, The University of Alabama, Tuscaloosa, Alabama 35487-0336, United States

Supporting Information

ABSTRACT: Reactions of ThO molecules and CH_4 have been investigated in solid argon near 4 K. The $CH_3Th(O)H$ molecule is produced when the sample is exposed to UV irradiation. Identification of this new intermediate is substantiated by observation of the Th═O and Th−H stretching vibrational modes with isotopic substitution via matrix infrared spectroscopy, and the assignments are supported by electronic structure frequency calculations. Methanol absorptions increase together with formation of the $CH_3Th(O)H$ molecule, suggesting a methane to methanol conversion induced by thorium oxide proceeding through the $CH_3Th(O)H$ intermediate. The formation of $CH_3Th(O)H$ from ThO + CH_4 is exothermic (ΔH_{rxn} = −11 kcal/mol) with an energy barrier of 30 kcal/mol at the CCSD(T)//B3LYP level. Decomposition of this intermediate to form methanol involves spin crossing, and the overall reaction from the intermediate is endothermic by 127 kcal/mol. There is no activation energy for the reaction of thorium atoms with methanol to give $CH_3Th(O)H$, as observed in separate experiments with Th and CH_3OH.

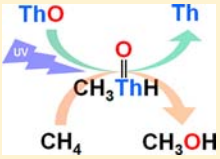

INTRODUCTION

The conversion from methane to methanol has attracted numerous studies since methanol can be widely used as a fuel as well as the starting material for producing other useful chemicals.[1] The successful partial oxidation of methane requires effective catalysts to break the inert C−H bond. A large number of studies have been performed on the preparation and optimization of homogeneous, heterogeneous and enzyme catalysts as well as probing the catalytic mechanisms.[2−5] In addition to these studies in the condensed phase, systematic gas phase studies using mass spectrometric methods have also been carried out in a wide range on the reactions of size-selected transition metal oxide ions toward methane as well as other hydrocarbons, as summarized in a series of recent reviews.[6−8] Although these studies were focused on simplified model molecular systems, valuable information on the mechanistic aspects can be obtained especially when combined with high level theoretical calculations.[9] Apart from the numerous studies in the gas phase employing charged species, the reactions of neutral transition metal oxide molecules and methane have received less attention, and most results are from spectroscopic studies in noble gas matrixes.[10] In particular, the cryogenic matrix environment makes it possible to relax and trap intermediates in the methane oxidation reaction, which are usually not accessible in the gas phase.[10]

Although reactions of neutral transition metal oxide molecules and methane have been systematically studied under matrix isolation conditions,[10−12] no investigation has been carried out on the reactivity of neutral actinide oxide species, even though the role of actinide elements in catalytic reactions has been the subject of many recent studies.[13,14] The most easily accessible actinide metals, uranium and thorium, have been shown to activate the C−H bonds of different hydrocarbons.[14,15] Gas phase mass spectrometric studies have provided detailed information on the reactivity and thermodynamics of actinide containing cations.[16] Recent experimental and theoretical studies on the reactions of thorium and uranium cations revealed that while thorium cations and dications reacted with CH_4 to form the $ThCH_2^+$ and $ThCH_2^{2+}$ products, no similar dehydrogenation reaction was observed for uranium cation owing to the endothermic character as well as the high energy barrier for the uranium reactions.[17−21]

Our recent matrix isolation infrared spectroscopic studies have provided evidence for the activation of methane by neutral uranium and thorium atoms, as the methylidene complexes CH_2MH_2 (M = U, Th) were observed. The computed structure of the uranium product is more distorted due to stronger agostic interactions.[22,23] For reactions involving uranium and thorium oxide cations in the gas phase, the oxide−arene adducts were the major products in most cases with H_2 and CH_4 elimination observed in a few cases depending on the reactant arenes.[16,24] The overall reaction efficiency for the actinide oxide cations was much lower than that for bare metal cations as evidenced by a series of reactivity studies with different hydrocarbons, and almost no reaction was observed between actinide oxide cations and methane.[18] In the current work, we report the reactions of laser-ablated neutral thorium oxide molecules and methane in solid argon at 4 K. Here, ThO molecules react with CH_4 when broad band UV irradiation is employed, which produces the $CH_3Th(O)H$ intermediate trapped in a solid argon matrix. At the same time, evidence is also provided for the formation of methanol, suggesting that the

Received: July 20, 2012
Published: September 24, 2012

   dx.doi.org/10.1021/ic301595h | *Inorg. Chem.* 2012, 51, 11055−11060

oxidation of methane proceeds in the presence of thorium oxide molecules.

EXPERIMENTAL AND THEORETICAL METHODS

The experimental apparatus and procedure for studying laser-ablated ThO and CH_4 reactions has been described previously.[25,26] The Nd:YAG laser fundamental (1064 nm, 10 Hz repetition rate with 10 ns pulse width) was focused onto a thorium dioxide (thoria ceramic) target mounted on a rotating rod. Laser-ablated thorium oxide materials, (ThO, Th, and O) were co-deposited with 4 mmol of argon (Matheson, research grade) containing 0.5% CH_4 (Matheson) onto a CsI cryogenic window at 4 K. Isotopic precursors CD_4 and $^{13}CH_4$ (Cambridge Isotope Laboratories, 99% enrichment) were used without purification. Complementary Th and methanol experiments also employed $CH_3{}^{18}OH$ (Cambridge Isotopic Laboratories, 95% enrichment). FTIR spectra were recorded at 0.5 cm^{-1} resolution on a Nicolet 750 FTIR instrument with HgCdTe range B detector. Matrix samples were annealed at different temperatures and cooled back to 4 K for spectral acquisition. Selected samples were subjected to broadband photolysis by a medium-pressure mercury arc street lamp (Philips, 175 W) with the outer pyrex globe removed to emit the entire quartz envelope output ($220 < \lambda < 900$ nm), which was also reduced using selected long wavelength pass optical glass filters.

Density functional theory (DFT)[27] with the B3LYP hybrid exchange−correlation functional[28] was used to optimize all of the structures. The initial calculations on $^1CH_3Th(O)H$ were done with the 6-311++G(d,p) basis set[29] on H, C, and O and the SDD effective core potential and basis set on Th.[30] (The preceding superscript in a formula corresponds to the usual spin state definition.) Subsequent calculations at the DFT/B3LYP level with the aug-cc-pVTZ[31] basis set on H, C, and O and the small core relativistic effective core potential (ECP) from the Stuttgart group[30,32] with the corresponding segmented [8s,7p,6d,4f,2g] basis set on Th were used to map out the potential energy surface. The Gaussian 09 program system was used for the optimization and frequency calculations of the minima and for the final DFT energies.[33] We were able to optimize some of the transition states using the options available for such optimizations in the Gaussian code.[34] In cases where we could not determine the transition state, we used the STEPPER approach with specific mode following in NWChem.[35] The DFT geometries were used in single point CCSD(T) calculations[36] performed with the MOLPRO 2010.1 program system[37] and with open shell molecules treated at the R/UCCSD(T) level.[38] The same ECP for Th was used as given above, but a larger basis set of the form [10s,9p,5d,4f,3g] was used following our previous work on ThO_2[39] with the aug-cc-pVTZ basis set on H, C, and O. We correlated[39] 12 valence electrons on Th in the CCSD(T) calculations (nominally the 6s, 6p, 7s, and 6d) and 6 electrons on O, 4 electrons on C, and 1 electron on each H atom.

RESULTS AND DISCUSSION

Infrared spectra from the reactions of laser-ablated thorium oxide materials (ThO, Th, and O) and methane in solid argon are shown in Figure 1. Strong absorption due to ThO, as well as weak ThO_2 bands were observed right after sample deposition (Figure 1, trace a), which result from laser ablation of the thorium oxide target. The yield of ThO in these experiments is much higher than that of ThO_2 relative to previous work with Th + O_2 reactions,[40] so we must conclude that either some ThO molecules survive ablation or that extensive recombination of the elements gives the high yield of ThO. In addition, the broad methyl radical absorption centered at 603 cm^{-1} (not shown here) was observed,[41] which is common in all of our reactions of laser-ablated metal atoms and methane, where the laser ablation plume photodissociates methane.[26] Trace absorptions were observed for two matrix trapping sites of CH_3OH at 1033.7 and 1027.0 cm^{-1} on sample deposition: these likely arise from reaction of laser-ablated O atoms with

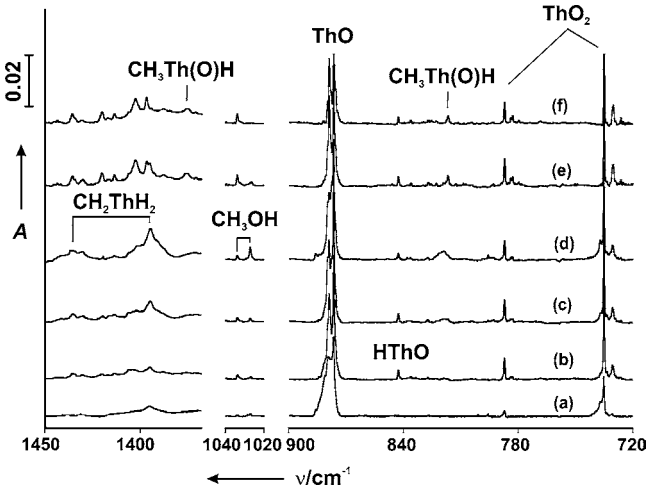

Figure 1. Infrared spectra of laser-ablated ThO, Th, and O and CH_4 reaction products in solid argon: (a) ThO + 0.5% CH_4 deposition for 60 min; (b) after annealing to 20 K; (c) after λ >290 nm irradiation; (d) after λ >220 nm irradiation; (e) annealing to 30 K; (f) after annealing to 35 K.

methane. Also weak bands at 1435.7, 1397.1, and 670.8 cm^{-1} due to the CH_2ThH_2 methylidene complex result from the reactions of thorium atoms and methane.[22] Subsequent sample annealing to 20 K increased the ThO_2 absorptions as well as a band at 842.6 cm^{-1} (Figure 1, trace b), which was assigned previously to the HThO molecule.[42] The CH_2ThH_2 bands increased and a new band pair was produced at 1370 and 817 cm^{-1} on exposure to pyrex filtered (λ > 290 nm) irradiation. When the sample was next exposed to full arc (λ > 220 nm) irradiation, the CH_2ThH_2 bands and the new pair at 1370 and 817 cm^{-1} increased along with the 1027.0 cm^{-1} matrix site band of the C−O stretching mode for CH_3OH. Together with the absorptions due to CH_2ThH_2, the 1370 and 817 cm^{-1} absorptions sharpened and shifted to 1375.5 and 816.7 cm^{-1} during sample annealing to 30 K but decreased slightly upon sample annealing to 35 K. After the absorption due to methanol increased at 1027.0 cm^{-1} upon UV irradiation, conversions between the two 1027.0 and 1033.7 cm^{-1} matrix site absorptions occurred during sample annealing (see Figure 1, traces d and e). Clearly, the increase of CH_3OH on full arc (λ > 220 nm) irradiation accompanies a further increase of the new pair of bands to be identified here.

Complementary studies of the reaction of thorium and methanol were also performed, and these showed similarities with the thorium oxide and methane reaction (Figure 2, trace d). The new band at 816.7 cm^{-1} appeared as well when the sample was annealed after sample deposition. However, the 1375.5 cm^{-1} band in the thorium and methanol experiment was not well resolved because of overlap with the methanol precursor absorptions.

A new product molecule resulting from the reaction of thorium oxide and methane must be considered since the 1375.5 and 816.7 cm^{-1} absorptions were not observed in reactions of thorium and methane. The 816.7 cm^{-1} band should be due to a terminal Th═O stretching mode due to the band position as well as the characteristic $^{16}O/^{18}O$ ratio of 1.0560 obtained from the Th and $CH_3{}^{18}OH$ reaction (Figure 2). Experiments with $^{13}CH_4$ revealed no ^{13}C shift for the 816.7 cm^{-1} band, and the reaction of thorium oxide and CD_4 resulted in a very small red shift of 1.8 cm^{-1}, which is comparable with

dx.doi.org/10.1021/ic301595h | Inorg. Chem. 2012, 51, 11055−11060

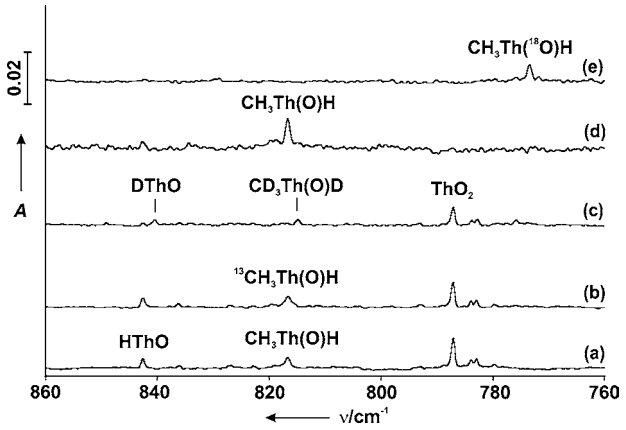

Figure 2. Infrared spectra of laser-ablated ThO, Th, and O and isotopically substituted CH_4 reaction products in solid argon (all spectra taken after λ >220 nm irradiation followed by annealing to 30 K): (a) ThO + 0.5% CH_4; (b) ThO + 0.5% $^{13}CH_4$; (c) ThO + 0.5% CD_4. (d, e) Infrared spectra of laser-ablated Th atoms and isotopically substituted CH_3OH reaction products in solid argon: (d) Th + 1.0% CH_3OH, after annealing to 35 K; (e) Th + 0.5% $CH_3{}^{18}OH$, after annealing to 40 K.

the 2.1 cm^{-1} red shift for the HThO molecule (Figure 2).[42] These observations suggest that this new terminal Th═O stretching mode is slightly perturbed by vibrational motions involving hydrogen. For the other band at 1375.5 cm^{-1}, an experiment with $^{13}CH_4$ gave no isotopic shift, indicating that carbon in the new molecule is not involved in this higher frequency vibrational mode. When CD_4 was used as the reactant, no band was observed between 1370 and 1450 cm^{-1}. This follows since absorptions in this region have been assigned to Th−H stretching modes of the CH_2ThH_2 molecule.[22] Hence it is also reasonable to assign the 1375.5 cm^{-1} band to the Th−H stretching mode of the new molecule. If the H/D isotopic ratio for the 1375.5 cm^{-1} band is similar to that of other Th−H containing species (1.39−1.40),[42] the deuterium counterpart would be observed in the region of 980−990 cm^{-1}; this is on the red side of the strong CD_4 absorption, which broadens upon sample annealing. On the basis of the two experimental frequencies, the new product molecule is identified as $CH_3Th(O)H$ with terminal Th═O and Th−H moieties.

Our assignment of this new molecule is strongly supported by calculations at the DFT/B3LYP level (Table 1). The $CH_3Th(O)H$ molecule is predicted to have a closed shell singlet ground state with a pyramidal geometry (Figure 3), similar to the recently characterized $CH_3U(O)H$ molecule.[43] The Th═O bond length and the corresponding stretching frequency for $CH_3Th(O)H$ are also close to those of the two previously characterized H_2ThO and $(CH_3)_2ThO$ molecules with Th(IV) centers.[42,44] The calculations predict two bands at 1397.2 and 834.8 cm^{-1} that are much stronger than all of the

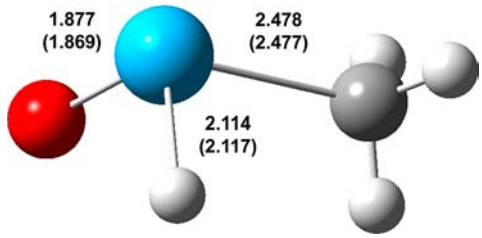

Figure 3. Structure of the ^1A ground state of the $CH_3Th(O)H$ molecule calculated at the B3LYP level of theory. Bond lengths in Å. Top numbers using the 6-311++G(d,p) + SDD basis set. Bond lengths and angles with the aug-cc-pVTZ + ECP basis set in parentheses: ∠OThH, 104.6° (104.8°); ∠CThH, 96.8° (96.8°); ∠CThO, 103.1° (103.2°); ∠sum = 304.5° (304.8°). Th is blue, O is red, C is gray, and H atoms are white.

other absorptions above 400 cm^{-1}. The Th−H harmonic stretching band predicted at 1397.2 cm^{-1} is slightly higher than the observed anharmonic frequency at 1375.5 cm^{-1}. The deuterium counterpart is calculated to be 993.4 cm^{-1} with only half of the intensity of the 1397.2 cm^{-1} band, in the region where the CD_4 precursor molecule absorbs. The Th−D band for the $CD_3Th(O)D$ molecule is probably covered by the strong CD_4 precursor band as noted above. For the calculated Th═O stretching mode at 834.8 cm^{-1}, the $^{16}O/^{18}O$ ratio is 1.0562. Both the band position and the isotopic frequency ratio agree well with the experimental results. We note that the calculated values are for the harmonic frequencies and the experimental values include anharmonic components as well as the influence of matrix atoms. These values reported to 0.1 cm^{-1} come from precise calculations and experiments, but one should not associate an error bar with the calculated frequencies to this accuracy.

In order to explore the reaction mechanism, the potential energy surface for the $^1ThO + CH_4 \rightarrow {}^3Th + CH_3OH$ reaction was calculated at the CCSD(T)//B3LYP level of theory (Figure 4) with the CCSD(T) energies including the B3LYP zero point energy correction. All of the singlet and triplet species except for the $^1ThO(CH_4)$ complex discussed below are shown. Formation of the $^1CH_3Th(O)H$ molecule from the reaction of ^1ThO and CH_4 is predicted to be exothermic (ΔH_{rxn} = −11 kcal/mol), with an energy barrier ($^1TS1$) of 30 kcal/mol separating reactants and the product. This modest energy barrier is consistent with the appearance of the $^1CH_3Th(O)H$ absorptions under broadband mercury arc UV irradiation. Geometry optimization of the $^1ThO(CH_4)$ complex resulted in separated ^1ThO and CH_4 at the DFT and MP2 levels, in agreement with the absence of the observation of this molecular complex in our experiments. $^3CH_3Th(O)H$ is predicted to be 56 kcal/mol above $^1CH_3Th(O)H$. Further decomposition of $^1CH_3Th(O)H$ is prohibited by energy barriers of 47 and 77 kcal/mol separating it from $^1CH_3ThOH$ and $^1CH_3OThH$ with the former being 24 kcal/mol more

Table 1. Observed and Calculated (in Bold) Infrared Absorptions (cm^{-1}) of the $CH_3Th(O)H$ Molecule in Solid Argon[a]

	CH_4	$^{13}CH_4$	CD_4	$CH_3{}^{18}OH$
Th−H str.	1375.5 **1397.2** (**479**)[c]	1375.5 **1397.2** (**479**)	[b] **993.4** (**224**)	1375.5 **1397.0** (**480**)
Th═O str.	816.7 **834.8** (**255**)[c]	816.7 **834.7** (**255**)	814.9 **832.4** (**263**)	773.4 **790.4** (**230**)

[a]Numbers in parentheses are infrared intensities in km/mol calculated at B3LYP level of theory. [b]Not observed due to band overlap. [c]When the larger aug-cc-pVTZ(ECP) basis set at the B3LYP level is used, the Th−H frequency is 1394.4 (477) cm^{-1} and the Th═O frequency is 845.2 (255) cm^{-1}.

dx.doi.org/10.1021/ic301595h | Inorg. Chem. 2012, 51, 11055−11060

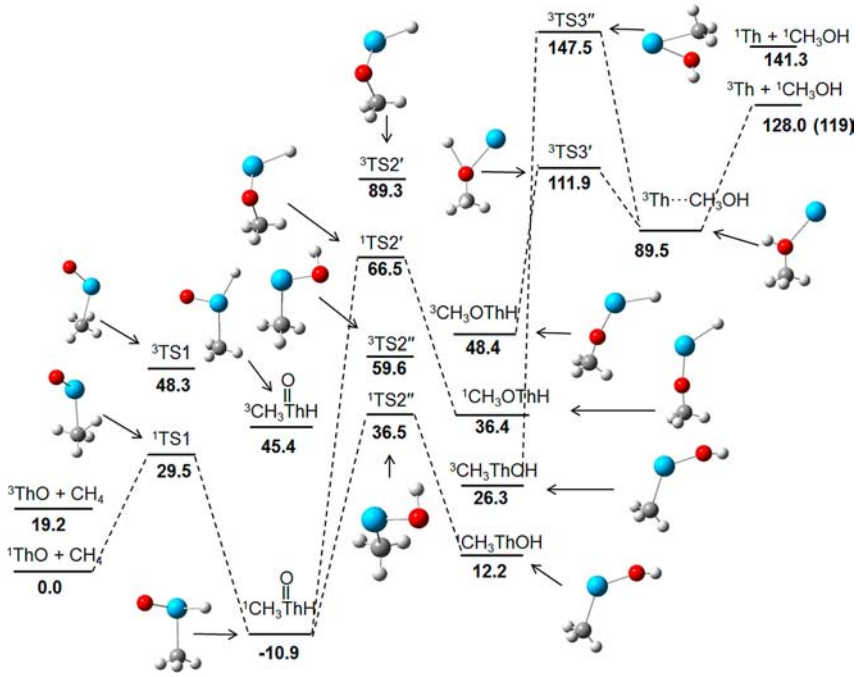

Figure 4. Calculated potential energy surface for the ^{1}ThO + CH_4 → ^{3}Th + CH_3OH reaction at the CCSD(T)/aug-cc-pVTZ(ECP)//B3LYP/aug-cc-pVTZ(ECP′) (see text for basis set details) level of theory in kcal/mol. The imaginary frequencies for the transition states are 1315*i* (^{1}TS1), 688*i* (^{3}TS1), 670*i* (^{1}TS2′), 1091*i* (^{3}TS2′), 1439*i* (^{1}TS2″), 466*i* (^{3}TS2″), 498*i* (^{3}TS3′), and 834*i* (^{3}TS3″). The spin−orbit corrected value for the ^{3}Th + $^1CH_3OH$ asymptote is in parentheses, and that for the ^{3}Th···CH_3OH complex is 81 kcal/mol.

stable than the latter. Both $^1CH_3ThOH$ and $^1CH_3OThH$ are predicted to be less stable than the reactant asymptote of ThO + CH_4. As observed in other divalent thorium species,[42,44,45] both the CH_3OThH and CH_3ThOH molecules have singlet ground states. $^3CH_3ThOH$ is predicted to be 14 kcal/mol higher than $^1CH_3ThOH$ and $^3CH_3OThH$ is predicted to be 12 kcal/mol above $^1CH_3OThH$. The presence of relatively small singlet−triplet splittings for Th (a heavy element) should enable spin orbit coupling in this region and crossing from the singlet to the triplet thereby allowing access to the lowest energy ^{3}Th + $^1CH_3OH$ product asymptote. The molecular singlet−triplet splitting is smaller than the ^{3}F−^{1}D splitting of 20.8 kcal/mol in the thorium atom, which is consistent with this hypothesis.[46]

The ^{3}Th + $^1CH_3OH$ asymptote is predicted to be 128 kcal/mol above the reactant asymptote ^{1}ThO + CH_4. Application of a spin orbit correction to the ^{3}Th atom ($\Delta E_{SO} = \sum_J[(2J + 1)\Delta E(J))]\sum_J[(2J + 1)]$) using the experimental spin orbit splittings[46] for the Th atom ($\Delta E(J)$) gives a reaction energy of 119 kcal/mol, which is in excellent agreement with the value of 118.7 ± 3.8 kcal/mol calculated from the experimental heats of formation.[47] A stable ^{3}Th···CH_3OH complex is 38 kcal/mol lower in energy than the product asymptote. This complex is separated by a 22 kcal/mol barrier from $^3CH_3OThH$, which is the higher energy isomer. The moderate barrier is due to the ease of hydrogen transfer. A much higher barrier of 58 kcal/mol separates the ^{3}Th···CH_3OH complex from the more stable isomer $^3CH_3ThOH$. The higher barrier is due to the difficulty in transferring the CH_3 group and actually lies above the ^{3}Th + $^1CH_3OH$ product asymptote. Since thorium atoms react spontaneously with methanol, it is most likely for the reaction to proceed through the higher energy $^3CH_3OThH$ isomer, which essentially requires no activation energy. A similar mechanism has been observed in the reactions of scandium and lanthanide atoms with methanol.[48] Our proposed pathway through the higher energy isomer with the lower barrier is also consistent with the fact that CH_3OH can be formed by broadband UV irradiation (Figure 1, trace d), where the UV energies applied in the experiment have approximately zero intensity at 220 nm (130 kcal/mol) and considerable intensity at 240 nm (119 kcal/mol). The energy of the 240 nm photon is just enough to overcome the endothermicity of the reaction from the stable intermediate to ^{3}Th + CH_3OH, and both photon energies are too low for the highest energy barrier to be accessed. This is consistent with the fact that lower energy >290 nm photolysis produces the $CH_3Th(O)H$ intermediate but *not additional* CH_3OH. All of the molecules on the potential energy surface prefer singlet ground states except for the ^{3}Th + CH_3OH asymptote and the ^{3}Th(CH_3OH) complex. This suggests that intersystem crossing occurs during the overall reaction, which is consistent with gas phase reactions involving transition metal oxide cations with high spin ground states.[6d,49]

Previous studies on the reactions of transition metal oxide molecules and methane revealed that $CH_3M(O)H$ intermediates were observed when laser-ablated TiO, NbO, and TaO molecules reacted with methane whereas the reactions of MnO and FeO with CH_4 gave the CH_3MOH products without metal−oxygen multiple bonds.[10] Formation of the $CH_3Th(O)H$ molecule further supports the similarity of thorium with the group IV metals, both of which have a highest oxidation state of IV, as is also displayed by the corresponding dioxides.[40,50] However, no ThO(CH_4) complex was observed in the thorium oxide experiments, which differs from the titanium case. It should be noted that TiO possesses a triplet ground state whereas the closed shell singlet is the most stable for the ThO molecule.[51] There is almost no reaction between ThO^+ cations and CH_4 from previous gas phase studies.[18] This reaction

dx.doi.org/10.1021/ic301595h | *Inorg. Chem.* 2012, 51, 11055−11060

profile should be different from that of the neutrals because the $CH_3Th(O)H^+$ cation will have a weaker Th−O bond energy with only three electrons available for that interaction rather than the four electrons available for neutral $CH_3Th(O)H$. Hence, the CH_3ThOH^+ cation with Th−C and Th−OH bonds or its decomposition products are expected to be formed, as observed in gas phase studies on the reactions of transition metal oxide cations with methane.[6]

CONCLUSION

Matrix isolated ThO molecules react with CH_4 to give the $CH_3Th(O)H$ product in solid argon at 4 K during UV irradiation. Infrared absorptions due to methanol also increased, along with the formation of $CH_3Th(O)H$ using full arc (λ > 220 nm) irradiation, suggesting a methane to methanol conversion induced by thorium oxide going through the $CH_3Th(O)H$ intermediate. Calculations at the B3LYP level reveal that the $CH_3Th(O)H$ molecule possesses a pyramidal structure with a closed shell singlet ground state. From the calculated potential energy surface, formation of the $CH_3Th(O)H$ molecule from the reaction of ThO and methane has an energy barrier of 30 kcal/mol and the $CH_3Th(O)H$ product is 11 kcal/mol more stable than the asymptotic reactants. Decomposition of this intermediate to $^3Th + CH_3OH$ is endothermic by 127 kcal/mol, and the formation of ^3Th will require a spin crossing. On the other hand, no activation energy is required for the reaction of ^3Th and methanol, which results in the spontaneous production of $^1CH_3Th(O)H$, again with a surface crossing needed. The reactions of thorium oxide and methane studied here suggest that actinide oxides such as ThO might be used to oxidize methane to methanol under photochemical conditions, analogous to transition metal oxide molecules.[10,11]

ASSOCIATED CONTENT

Supporting Information

Complete references 33 and 37 and tables containing thermochemical values at the CCSD(T) and B3LYP level of theory, frequencies and IR intensities at the B3LYP level of theory for $^1CH_3Th(O)H$, $^1CH_3ThOH$, and $^1CH_3OThH$ and optimized B3LYP Cartesian coordinates for the various structures. This material is available free of charge via the Internet at http://pubs.acs.org.

AUTHOR INFORMATION

Corresponding Author

*E-mail: lsa@virginia.edu (L.A.); dadixon@as.ua.edu (D.A.D.).

Notes

The authors declare no competing financial interest.

ACKNOWLEDGMENTS

We gratefully acknowledge financial support from DOE Office of Science, Basic Energy Supported by DOE Grant DE-SC0001034 (L.A.) and the BES SISGR program in actinide sciences (D.A.D.).

REFERENCES

(1) Holmen, A. *Catal. Today* **2009**, *142*, 2−8.
(2) Hashiguchi, B. G.; Hoevelmann, C. H.; Bischof, S. M.; Lokare, K. S.; Leung, C. H.; Periana, R. A. In *Methane to Methanol Conversion. Energy Production and Storage: Inorganic Chemical Strategies for a Warming World*; Crabtree, R. H., Ed.; Wiley: New York, 2010; p 101.
(3) Gunay, A.; Theopold, K. H. *Chem. Rev.* **2010**, *110*, 1060−1081.
(4) Vanelderen, P.; Hadt, R. G.; Smeets, P. J.; Solomon, E. I.; Schoonheydt, R. A.; Sels, B. F. *J. Catal.* **2011**, *284*, 157−164.
(5) Himes, R. A.; Barnese, K.; Karlin, K. D. *Angew. Chem., Int. Ed.* **2010**, *49*, 6714−6716.
(6) (a) Böhme, D. K.; Schwarz, H. *Angew. Chem., Int. Ed.* **2005**, *44*, 2336−2354. (b) Schröder, D.; Schwarz, H. *Proc. Natl. Acad. Sci. U.S.A.* **2008**, *105*, 18114−18119. (c) Schlangen, M.; Schwarz, H. *Dalton Trans.* **2009**, 10155−10165. (d) Schwarz, H. *Angew. Chem., Int. Ed.* **2011**, *50*, 10096−10115. (e) Dietl, N.; Schlangen, M.; Schwarz, H. *Angew. Chem., Int. Ed.* **2012**, *51*, 5544−5555.
(7) (a) Johnson, G. E.; Tyo, E. C.; Castleman, A. W., Jr. *Proc. Natl. Acad. Sci. U.S.A.* **2008**, *105*, 18108−18113. (b) Johnson, G. E.; Mitrić, R.; Bonačić-Koutecký, V.; Castleman, A. W., Jr. *Chem. Phys. Lett.* **2009**, *475*, 1−9. (c) Irikura, K. K.; Beauchamp, J. L. *J. Am. Chem. Soc.* **1989**, *111*, 75−85.
(8) (a) Yin, S.; Bernstein, E. R. *Int. J. Mass Spectrom.* **2012**, *321*−*322*, 49−65. (b) Zhao, Y. X.; Wu, X. N.; Ma, J. B.; He, S. G.; Ding, X. L. *Phys. Chem. Chem. Phys.* **2011**, *13*, 1925−1938. (c) Ding, X. L.; Wu, X. N.; Zhao, Y. X.; He, S. G. *Acc. Chem. Res.* **2012**, *45*, 382−390. (d) Operti, L.; Rabezzana, R. *Mass Spectrom. Rev.* **2006**, *25*, 483−513.
(9) Roithová, J.; Schröder, D. *Chem. Rev.* **2010**, *110*, 1170−1211.
(10) Wang, G. J.; Zhou, M. F. *Int. Rev. Phys. Chem.* **2008**, *27*, 1−25.
(11) Wang, G. J.; Gong, Y.; Chen, M. H.; Zhou, M. F. *J. Am. Chem. Soc.* **2006**, *128*, 5974−5980.
(12) (a) Wang, G. J.; Chen, M. H.; Zhou, M. F. *J. Phys. Chem. A* **2004**, *108*, 11273−11278. (b) Wang, G. J.; Lai, S. X.; Chen, M. H.; Zhou, M. F. *J. Phys. Chem. A* **2005**, *109*, 9514−9520.
(13) (a) Andrea, T.; Eisen, M. S. *Chem. Soc. Rev.* **2008**, *37*, 550−567. (b) Barnea, E.; Eisen, M. S. *Coord. Chem. Rev.* **2006**, *250*, 855−899.
(14) Fox, A. R.; Bart, S. C.; Meyer, K.; Cummins, C. C. *Nature* **2008**, *455*, 341−349.
(15) Pool, J. A.; Scott, B. L.; Kiplinger, J. L. *J. Am. Chem. Soc.* **2005**, *127*, 1338−1339.
(16) (a) Gibson, J. K. *Int. J. Mass Spectrom.* **2002**, *214*, 1−21. (b) Gibson, J. K.; Marcalo, J. *Coord. Chem. Rev.* **2006**, *250*, 776−783. (c) Gibson, J. K.; Haire, R. G.; Marcalo, J.; Santos, M.; Leal, J. P.; Pires de Matos, A.; Tyagi, R.; Mrozik, M. K.; Pitzer, R. M.; Bursten, B. E. *Eur. Phys. J. D* **2007**, *45*, 133−138.
(17) Di Santo, E.; Santos, M.; Michelini, M. C.; Marcalo, J.; Russo, N.; Gibson, J. K. *J. Am. Chem. Soc.* **2011**, *133*, 1955−1970.
(18) Gibson, J. K.; Haire, R. G.; Marcalo, J.; Santos, M.; Pires de Matos, A.; Mrozik, M. K.; Pitzer, R. M.; Bursten, B. E. *Organometallics* **2007**, *26*, 3947−3956.
(19) (a) Heinemann, C.; Cornehl, H. H.; Schwarz, H. *J. Organomet. Chem.* **1995**, *501*, 201−209. (b) Armentrout, P. B.; Hodges, R. V.; Beauchamp, J. L. *J. Chem. Phys.* **1977**, *66*, 4683−4688.
(20) Marcalo, J.; Leal, J. P.; Pires de Matos, A. *Int. J. Mass Spectrom. Ion Processes* **1996**, *157*/*158*, 265−274.
(21) (a) Di Santo, E.; Michelini, M. d. C.; Russo, N. *Organometallics* **2009**, *28*, 3716−3726. (b) de Almeida, K. J.; Duarte, H. A. *Organometallics* **2010**, *29*, 3735−3745. (c) de Almeida, K. J.; Duarte, H. A. *Organometallics* **2009**, *28*, 3203−3211. (d) de Almeida, K. J.; Cesar, A. *Organometallics* **2006**, *25*, 3407−3416.
(22) Andrews, L.; Cho, H. G. *J. Phys. Chem. A* **2005**, *109*, 6796−6798.
(23) Lyon, J. T.; Andrews, L.; Malmqvist, P. Å.; Roos, B. O.; Yang, T.; Bursten, B. E. *Inorg. Chem.* **2007**, *46*, 4917−4925.
(24) Marcalo, J.; Leal, J. P.; Pires de Matos, A. *Organometallics* **1997**, *16*, 4581−4588.
(25) (a) Andrews, L.; Citra, A. *Chem. Rev.* **2002**, *102*, 885−911. (b) Andrews, L. *Chem. Soc. Rev.* **2004**, *33*, 123−132.
(26) (a) Andrews, L.; Cho, H. G. *Organometallics* **2006**, *25*, 4040−4053. (b) Cho, H. G.; Wang, X. F.; Andrews, L. *J. Am. Chem. Soc.* **2005**, *127*, 465−473.
(27) Parr, R. G.; Yang, W. *Density-Functional Theory of Atoms and Molecules*; Oxford Univ. Press: Oxford, 1989.
(28) (a) Becke, A. D. *J. Chem. Phys.* **1993**, *98*, 5648−5652. (b) Lee, C.; Yang, W.; Parr, R. G. *Phys. Rev. B* **1988**, *37*, 785−789.

(29) Frisch, M. J.; Pople, J. A.; Binkley, J. S. *J. Chem. Phys.* **1984**, *80*, 3265−3269.
(30) Kuechle, W.; Dolg, M.; Stoll, M. H.; Preuss, H. *J. Chem. Phys.* **1994**, *100*, 7535−7542.
(31) Kendall, R. A.; Dunning, T. H., Jr.; Harrison, R. J. *J. Chem. Phys.* **1994**, *96*, 6796−6806.
(32) (a) Institut für Theoretische Chemie Universität Stuttgart, http://www.theochem.uni-stuttgart.de/pseudopotentials/index.en.html. (b) Cao, X.; Dolg, M.; Stoll, H. *J. Chem. Phys.* **2003**, *118*, 487−496. (c) Cao, X.; Dolg, M. *J. Mol. Struct. (Theochem)* **2004**, *673*, 203−209.
(33) Frisch, M. J.; et al. *Gaussian 09*; Gaussian, Inc.: Wallingford, CT, 2009.
(34) (a) Peng, C.; Schlegel, H. B. *Isr. J. Chem.* **1993**, *33*, 449−454. (b) Peng, C.; Ayala, P. Y.; Schlegel, H. B.; Frisch, M. J. *J. Comput. Chem.* **1996**, *17*, 49−56.
(35) (a) Valiev, M.; et al. *Comput. Phys. Commun.* **2010**, *181*, 1477−1489. (b) Kendall, R. A.; et al. *Comput. Phys. Commun.* **2000**, *128*, 260−283.
(36) Bartlett, R. J.; Musial, M. *Rev. Mod. Phys.* **2007**, *79*, 291−352.
(37) Knowles, P. J.; Manby, F. R.; Schütz, M.; Celani, P.; Knizia, G.; Korona, T.; Lindh, R.; Mitrushenkov, A.; Rauhut, G.; Adler, T. B.; et al., MOLPRO, version 2010.1, a package of ab initio programs, see http://www.molpro.net.
(38) (a) Deegan, M. J. O.; Knowles, P. J. *Chem. Phys. Lett.* **1994**, *227*, 321−327. (b) Knowles, P. J.; Hampel, C.; Werner, H. J. *J. Chem. Phys.* **1993**, *99*, 5219−5227. (c) Rittby, M.; Bartlett, R. J. *J. Phys. Chem.* **1988**, *92*, 3033−3036.
(39) Jackson, V. E.; Craciun, R.; Dixon, D. A.; Peterson, K. A.; de Jong, W. A. *J. Phys. Chem. A* **2008**, *112*, 4095−4099.
(40) Andrews, L.; Gong, Y.; Liang, B.; Jackson, V. E.; Flamerich, R.; Li, S.; Dixon, D. A. *J. Phys. Chem. A* **2011**, *115*, 14407−14416.
(41) Jacox, M. E. *J. Mol. Spectrosc.* **1977**, *66*, 272−287.
(42) Liang, B. Y.; Andrews, L.; Li, J.; Bursten, B. E. *J. Am. Chem. Soc.* **2002**, *124*, 6723−6733.
(43) Gong, Y.; Andrews, L. *Inorg. Chem.* **2011**, *50*, 7099−7105.
(44) Gong, Y.; Andrews, L. *Dalton Trans.* **2011**, *40*, 11106−11114.
(45) Wang, X. F.; Andrews, L. *Phys. Chem. Chem. Phys.* **2005**, *7*, 3834−3838.
(46) Blaise, J.; Wyart, J. F. Energy Levels and Atomic Spectra of Actinides, Int'l Tables of Selected Constants **20**, Tables de Constantes, Paris (1992). http://www.nist.gov/pml/data/handbook/index.cfm. Sansonetti, J. E.; Martin, W. C. *J. Phys. Chem. Ref. Data.* **2005**, *34*, 1559−2259.
(47) (a) Konigs, R. J. M.; Benes, O. J. *J. Phys. Chem. Ref. Data* **2010**, *39*, No. 043102. (b) Konigs, R. J. M.; Morss, L. R.; Fuger, J. In *The Chemistry of the Actinide and Transactinide Elements*, 3rd ed.; Morss, L. R., Edelstein, N. M., Fuger, J., Eds.; Springer: Dordrecht, the Netherlands, 2006; Vol. *4*, Chapter 19, pp 2113−2224. (c) Cox, J. D.; Wagman, D. D.; Medvedev, V. A. *CODATA Key Values for Thermodynamics*, Hemisphere: New York, 1989. (d) Chase, M. W., Jr. *NIST-JANAF Thermochemical Tables*, 4th ed.; Journal of Physical and Chemical Reference Data, Monograph 9; American Institute of Physics: Woodbury, NY, 1998; Suppl. 1.
(48) (a) Gong, Y.; Andrews, L.; Chen, M. Y.; Dixon, D. A. *J. Phys. Chem. A* **2011**, *115*, 14581−14592. (b) Chen, M. H.; Huang, Z. G.; Zhou, M. F. *J. Phys. Chem. A* **2004**, *108*, 5950−5955.
(49) Schröder, D.; Shaik, S.; Schwarz, H. *Acc. Chem. Res.* **2000**, *33*, 139−145.
(50) Chertihin, G. V.; Andrews, L. *J. Phys. Chem.* **1995**, *99*, 6356−6366.
(51) Gong, Y.; Zhou, M. F.; Andrews, L. *Chem. Rev.* **2009**, *109*, 6765−6808.